Human Immunodeficiency Virus Type 1 and Methamphetamine-Mediated Mitochondrial Damage and Neuronal Degeneration in Human Neurons

Carmen Teodorof-Diedrich,[a] Stephen A. Spector[a,b]

[a]Department of Pediatrics, Division of Infectious Diseases, University of California San Diego, La Jolla, California, USA
[b]Rady Children's Hospital, San Diego, California, USA

ABSTRACT Methamphetamine, a potent psychostimulant, is a highly addictive drug commonly used by persons living with HIV (PLWH), and its use can result in cognitive impairment and memory deficits long after its use is discontinued. Although the mechanism(s) involved with persistent neurological deficits is not fully known, mitochondrial dysfunction is a key component in methamphetamine neuropathology. Specific mitochondrial autophagy (mitophagy) and mitochondrial fusion and fission are protective quality control mechanisms that can be dysregulated in HIV infection, and the use of methamphetamine can further negatively affect these protective cellular mechanisms. Here, we observed that treatment of human primary neurons (HPNs) with methamphetamine and HIV gp120 and Tat increase dynamin-related protein 1 (DRP1)-dependent mitochondrial fragmentation and neuronal degeneration. Methamphetamine and HIV proteins increased microtubule-associated protein 1 light chain 3 beta-II (LC3B-II) lipidation and induced sequestosome 1 (SQSTM1, p62) translocation to damaged mitochondria. Additionally, the combination inhibited autophagic flux, increased reactive oxygen species (ROS) production and mitochondrial damage, and reduced microtubule-associated protein 2 (MAP2) dendrites in human neurons. *N*-Acetylcysteine (NAC), a strong antioxidant and ROS scavenger, abrogated DRP1-dependent mitochondrial fragmentation and neurite degeneration. Thus, we show that methamphetamine combined with HIV proteins inhibits mitophagy and induces neuronal damage, and NAC reverses these deleterious effects on mitochondrial function.

IMPORTANCE Human and animal studies show that HIV infection, combined with the long-term use of psychostimulants, increases neuronal stress and the occurrence of HIV-associated neurocognitive disorders (HAND). On the cellular level, mitochondrial function is critical for neuronal health. In this study, we show that in human primary neurons, the combination of HIV proteins and methamphetamine increases oxidative stress, DRP1-mediated mitochondrial fragmentation, and neuronal injury manifested by a reduction in neuronal network and connectivity. The use of NAC, a potent antioxidant, reversed the neurotoxic effects of HIV and methamphetamine, suggesting a novel approach to ameliorate the effects of HIV- and methamphetamine-associated cognitive deficits.

KEYWORDS HIV gp120, HIV Tat, human primary neurons, mitochondrial fragmentation, mitochondrial damage, MAP2 neuronal dendrites, reactive oxygen species, NAC

Despite the progress in human immunodeficiency virus type-1 (HIV-1) treatment through combination antiretroviral therapy (ART), mild neurocognitive impairment remains an important HIV-associated clinical problem for 10 to 25% of persons living

with HIV (PLWH) (1). HIV enters the central nervous system (CNS) during the initial stages of infection and can cause neurological dysfunction (2). The dissemination of HIV proteins gp120 and Tat from infected cells is believed to play a principal role in HIV-associated neurocognitive disorders (HAND). However, the mechanism(s) leading to neurological impairment remains poorly understood (3). In addition to the direct effects of HIV and its components, some antiretrovirals used to suppress the virus and substance use, including methamphetamine (METH), are thought to contribute to HAND (4).

Autophagy is a highly regulated protective mechanism responsible for clearance of excessive or damaged proteins and cellular organelles by lysosomes (5). Dysregulation of autophagy has been identified by our group and others in human brains and animal models of HAND (6–10). Accumulating evidence indicates that specific elimination of damaged mitochondria through autophagy (mitophagy) and mitochondrial dynamics play important roles in CNS diseases (10, 11). We have previously shown that human primary neurons (HPNs) treated with HIV gp120 and Tat viral proteins exhibit dysregulated mitochondrial dynamics with enhanced fragmentation mediated by dynamin-related protein 1 (DRP1) mitochondrial translocation. HIV proteins increased Parkin translocation to the damaged mitochondria but mediated incomplete delivery of mitochondria to the lysosomal compartment and blockage of the mitophagic flux (10). Neuronal cells are sensitive to impaired autophagy, and the degradation and recycling of damaged mitochondria through mitophagy are critical to proper neuronal function (11). Dysfunctional mitochondria are a source of reactive oxygen species (ROS), and mitochondrial depolarization and neuritic beading are early signs of neuronal toxicity present under pathological conditions, including HAND (12, 13). Increasing evidence indicates that HIV infection and methamphetamine use can potentiate mitochondrial injury in neurons and contribute to neurocognitive morbidity (14). Methamphetamine-induced mitochondrial fragmentation and ROS production were reported in a rat hippocampal neural progenitor cell model and provided a potential mechanism for methamphetamine-related neurodegenerative disorders (15). Methamphetamine has also been found to potentiate HIV gp120-mediated autophagy in astrocytes, and long-term treatment with methamphetamine in combination with gp120 induced astrocyte cell death (16). Methamphetamine treatment of HIV gp120 transgenic mice revealed increased neuronal injury, loss of neuronal dendrites, and long-lasting pre-synaptic and postsynaptic alterations which resulted in impaired learning and memory (17). In the current research, we hypothesized that altered mitochondrial dynamics and autophagy associated with HIV infection and methamphetamine use would increase cellular oxidative stress and subsequently mitochondrial damage and neuronal injury, factors that could play an important role in the development of HAND and the advanced aging associated with HIV infection. Our findings demonstrate that in human primary neurons, gp120 and Tat in combination with methamphetamine induce the disruption of the mitochondrial network, resulting in mitochondrial fragmentation, oxidative stress, ROS production, and neuronal degeneration. Moreover, *N*-acetylcysteine (NAC), a potent antioxidant, abrogated DRP1-induced mitochondrial fragmentation and neuronal degeneration.

RESULTS

Methamphetamine increases LC3B-II lipidation and dysregulates autophagic flux in HIV-exposed neurons. Autophagy is a highly regulated catabolic process important for cell survival (18). Multiple studies have shown that HIV proteins can interfere with autophagic and mitophagic pathways that are linked to neurodegeneration (6, 7, 10, 19). Our initial experiments were designed to determine if methamphetamine altered autophagy in primary neurons. The concentrations of methamphetamine used were chosen based on preliminary studies showing that in binge users methamphetamine is a lipid-soluble molecule easily distributed and retained in the brain where it can reach a concentration of up to 200 to 1,040 μM (20, 21). For our initial studies, HPNs were exposed to increasing concentrations of methamphetamine for 24 h, and
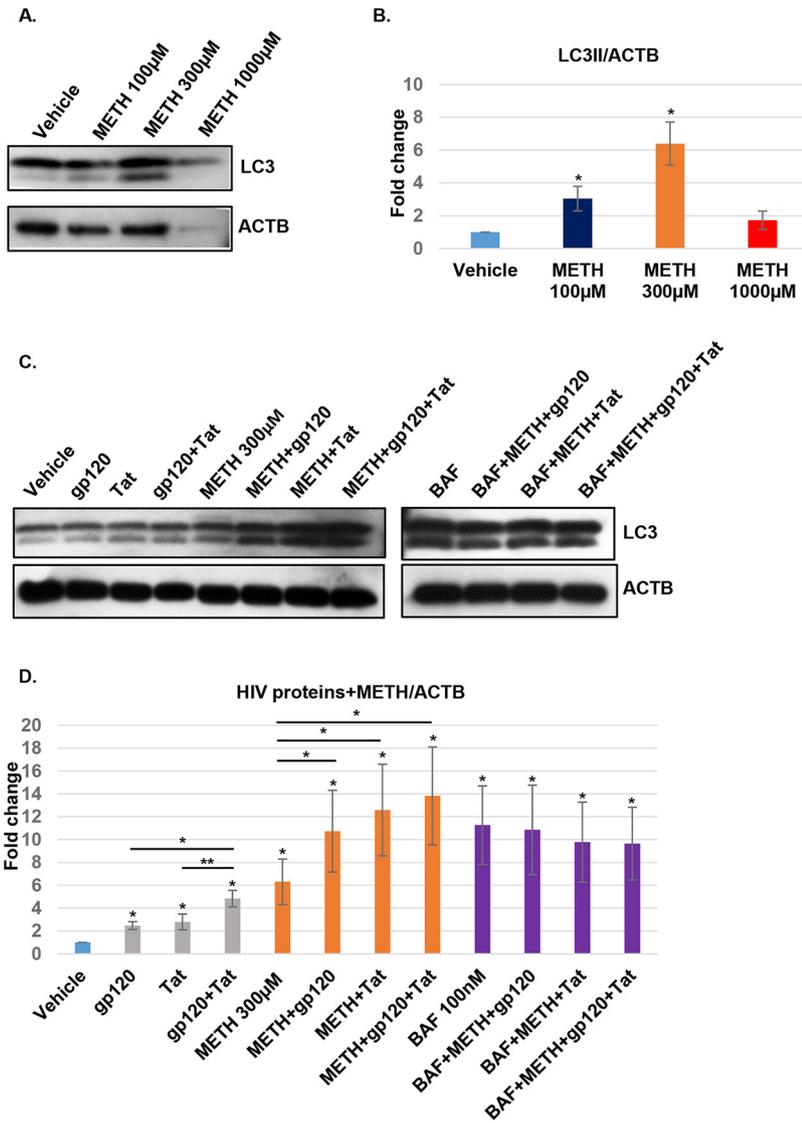
FIG 1 HIV and methamphetamine increase LC3B-II and block autophagic flux. (A and B) Methamphet-amine (METH) dose-dependent treatment. Cell lysates were extracted with mitochondrial lysis buffer, clarified by centrifugation, and analyzed by Western blotting using antibodies against LC3B-II. Beta-actin (ACTB) was used as an internal control. The relative expression of LC3B-II was normalized to that of beta-actin and analyzed by ImageJ software. Data are represented as means ± standard deviations ($n = 3$, $P < 0.05$). (C and D) LC3B-II protein expression was analyzed in cell lysates treated with gp120, Tat, gp120 and Tat, methamphetamine, or combinations of these for 24 h and with 100 nM bafilomycin A1 (BAFA1) for 8 h prior to collection. Beta-actin was used as an internal loading control. The relative expression of LC3B-II was normalized to that of beta-actin and analyzed by ImageJ software. Student's t test was performed to test the statistical significance. Data are presented as mean values ± standard deviations ($n = 3$ independent donors). *, $P < 0.05$; **, $P < 0.01$.

proteins were extracted and assessed for light chain 3 beta-II (LC3B-II) expression by Western blotting. HPNs responded to methamphetamine treatment in a dose-dependent manner, with a concentration of 100 μM resulting in a mean 3.04-fold increase in LC3B-II lipidation ($P < 0.05$); methamphetamine at 300 μM showed the maximum increase in LC3B-II expression (6.39-fold increase; $P < 0.05$) (Fig. 1A and B).

In previous studies, we showed that HIV gp120 and Tat block autophagic flux in human neurons (10). To determine if methamphetamine alters the effect of HIV proteins on autophagy, neurons were treated with 100 ng/ml HIV gp120, Tat, or a combination of the two in the presence or absence of 300 μM methamphetamine for 24 h and with 100 nM bafilomycin A1 (BAFA1) for 8 h (Fig. 1C). A mean fold increase of
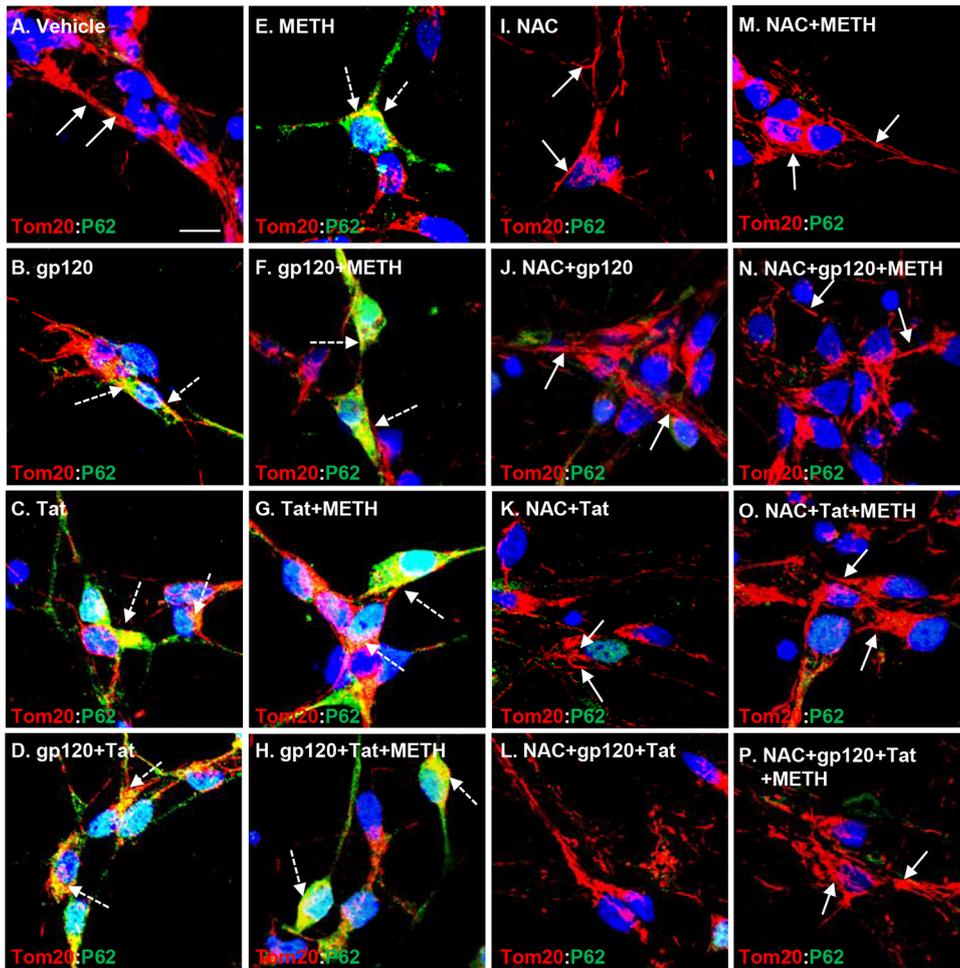
FIG 2 HIV and methamphetamine increase p62 translocation to the damaged mitochondria. (A) In vehicle-treated cells, confocal laser microscopy analysis shows low and diffuse cytoplasmic expression and association of p62 with TOM20-stained mitochondria (indicated by the white arrows). (B to H) Confocal laser microscopy analysis shows increased expression, translocation, and colocalization of p62 with TOM20-stained mitochondria (indicated by the dashed white arrows) in HIV-, methamphetamine-, or combination-treated cells. (I to P) NAC (1 mM) pretreatment abrogated increased p62 expression and translocation to the mitochondria in HIV-, methamphetamine-, or combination-treated cells. Nuclei were stained with 4′,6′-diamidino-2-phenylindole (blue). Scale bar, 10 μm.

2.4, 2.7, and 4.8 in LC3B-II lipidation was observed for gp120, Tat, and the combination, respectively ($P < 0.05$ for all comparisons to the control). Methamphetamine alone or in combination with HIV proteins resulted in a mean fold increase of 6.2, 10.7, 12.5, and 13.8, respectively ($P < 0.05$ for all comparisons to the control). However, no increase in LC3B-II was observed in the presence of BAFA1, methamphetamine, and HIV proteins compared to levels with BAFA1 treatment alone (P is nonsignificant [ns]) (Fig. 1C and D), indicating that HIV and methamphetamine block autophagic flux and induce neuronal dysfunction.

Methamphetamine increases p62 translocation and association to damaged mitochondria in HIV-treated neurons. Exposure of brain cells to HIV proteins has been shown to increase the expression and translocation of p62 to mitochondria, followed by inhibition of autophagic flux and accumulation of autophagosomes (10, 22). Therefore, we next examined the combined effect of methamphetamine and HIV proteins on p62 translocation and recruitment to the perinuclear area where damaged mitochondria are present. An increase in expression and association of p62 to TOM20-labeled mitochondria was observed in the presence of HIV proteins and methamphetamine that was enhanced in the presence of both, suggesting that methamphetamine further increases p62/TOM20 complex formation in HIV-treated human neurons (Fig. 2A

to H). In contrast, pretreatment with 1 mM NAC, a potent antioxidant, for 1 h followed by HIV and methamphetamine treatment for 24 h abrogated immune association of p62 and TOM20 and reversed protein expressions to the basal levels (Fig. 2I to P). These results suggest that treatment of neurons with HIV proteins and methamphetamine upregulated the expression of p62 and increased its translocation to the perinuclear area where damaged mitochondria are present. NAC pretreatment abrogated the effects of HIV and methamphetamine on the upregulation of autophagic proteins.

Methamphetamine increases mitochondrial fragmentation in HIV-treated neurons. HIV proteins are thought to promote mitochondrial dysfunction and alter mitochondrial morphology and dynamics in infected brains (10, 23–25). Mitochondrial fragmentation is an early event that precedes neuronal degeneration mediated by oxidative stress and neurotoxin production (26). Similarly, methamphetamine-induced mitochondrial fragmentation has been reported in rat neural progenitor cells (15). Therefore, we hypothesized that methamphetamine in combination with HIV proteins would significantly alter mitochondrial dynamics in human neurons and increase mitochondrial fragmentation. HPNs were treated with 100 ng/ml gp120, Tat, or both proteins in the presence or absence of 300 μM methamphetamine for 24 h. Neuronal mitochondria were stained using TOM20 antibody. Confocal microscopy analysis identified mitochondrial aggregation and fragmentation in HIV- and methamphetamine-treated neuronal cells (Fig. 3A to E), a process exacerbated when HIV proteins and methamphetamine were combined (Fig. 3A, F, G, and H).

Since ROS production can lead to mitochondrial fragmentation dysfunction (27), we examined whether NAC has a neuroprotective effect (28). HPNs were pretreated with 1 mM NAC for 1 h, followed by exposure to HIV proteins and methamphetamine for 24 h (Fig. 3I to P). NAC pretreatment of HIV- and methamphetamine-exposed neurons abrogated mitochondrial fragmentation (Fig. 3I to P). HPN mitochondrial size as determined by Fiji (ImageJ) (Fig. 3R) software significantly decreased for all HIV proteins and methamphetamine exposures ($P < 0.05$ for all comparisons to the control), with the greatest reduction in size occurring when HIV proteins were combined with methamphetamine. When cells were pretreated with NAC, mitochondrial size no longer differed from that of the control for each HIV protein and methamphetamine when used singly or in combination ($P > 0.05$ for all comparisons) (Fig. 3R).

Methamphetamine increases mitochondrial fragmentation through DRP1 translocation in HIV-treated neurons. Mitochondrial dynamics regulates mitochondrial morphology, distribution, and function. The balance between fusion and fission is regulated by key proteins (29, 30) including dynamin-related protein 1 (DRP1), a GTPase that controls mitochondrial fragmentation (31). We have shown previously that HIV proteins gp120 and Tat trigger DRP1-mediated mitochondrial fragmentation in HPNs, with increased expression and translocation of DRP1 to damaged mitochondria (10). Furthermore, DRP1 has been shown to be involved in the regulation of methamphetamine-mediated mitochondrial fragmentation in neural progenitor cells (15). Thus, it was important to assess if HIV and methamphetamine further regulate DRP1 expression and translocation to mitochondria in HPNs. Following exposure to HIV proteins and methamphetamine, DRP1 expression and translocation to mitochondria increased under all conditions. At 24 h, treatment with gp120 alone and methamphetamine alone resulted in mean 3.5-fold and 4.9-fold increases in DRP1 expression, respectively ($P < 0.05$ for all comparisons to control) (Fig. 4A and B). The combination of gp120 and methamphetamine induced a mean 6.3-fold increase in DRP1 expression ($P < 0.01$), and NAC pretreatment abrogated DRP1 expression to the levels similar to those for cells treated with vehicle and NAC only ($P =$ ns for all comparisons to controls) (Fig. 4A and B). In the same manner, treatment with Tat alone and methamphetamine alone resulted in mean 2.8-fold and 4.7-fold increases in DRP1 expression, respectively ($P < 0.03$ for all comparisons to control), and Tat in combination with methamphetamine induced a mean 6.2-fold increase in DRP1 expression ($P < 0.01$) (Fig. 4C and D). NAC pretreatment in Tat- and methamphetamine-exposed neurons reduced DRP1 expression to levels equivalent to those of the controls ($P =$ ns) (Fig. 4C and D). A mean
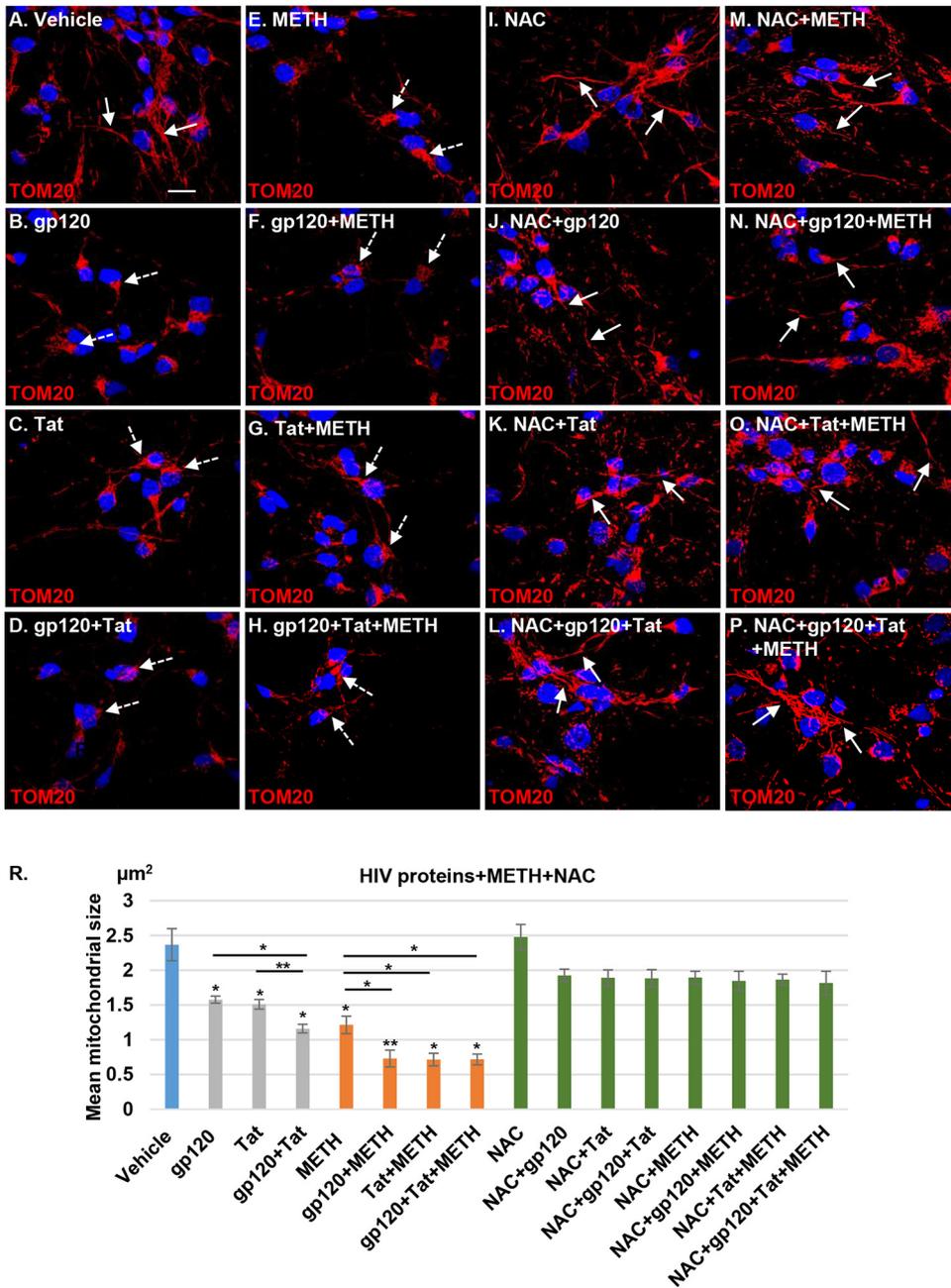
FIG 3 Methamphetamine increases mitochondrial fragmentation in HIV-treated human neurons. (A) Confocal laser microscopy analysis showing healthy tubular mitochondrial structures (indicated by the white arrows) in vehicle-treated cells. (B to H) Treatment for 24 h with 100 ng/ml gp120, Tat, or gp120/Tat and 300 μM methamphetamine alone or in combination with HIV proteins. Confocal microscopy shows mitochondrial aggregation and fragmentation (indicated by the dashed white arrows). Mitochondria were stained with TOM20 (red); nuclei were stained with 4′,6′-diamidino-2-phenylindole (blue). (I to P) NAC (1 mM) pretreatment followed by HIV, methamphetamine, and combination treatment in neuronal cells. Confocal microscopy shows recovery of the mitochondrial morphology and network. (R) Quantitative analysis of mitochondrial size using ImageJ-Fiji software. Student's t test was performed to test the statistical significance. Data are presented as mean values $\pm$ standard deviations ($n = 3$ independent donors). *, $P < 0.05$; **, $P < 0.01$. Scale bar, 10 μm.

fold increase of 6.2, 6.5, or 9.07 in DRP1 expression was observed for gp120 and Tat, methamphetamine, and the combination treatment, respectively ($P < 0.01$ for all comparisons to the control) (Fig. 4E and F); NAC pretreatment reduced DRP1 expression to values similar to those of control-treated cells ($P = $ ns) (Fig. 4E and F).

We next examined by confocal microscopy if HIV proteins in combination with methamphetamine showed increased DRP1 translocation in the perinuclear area in
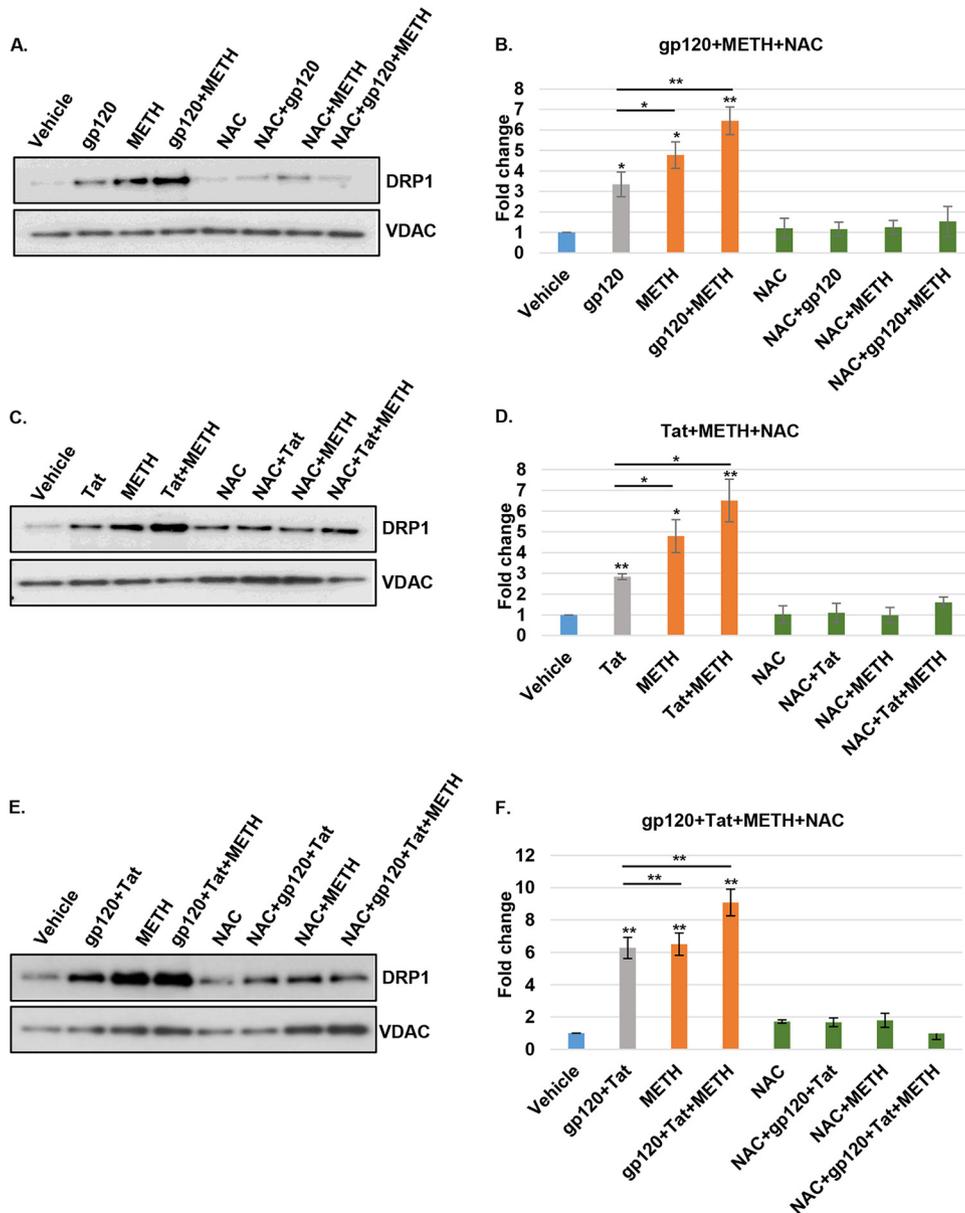
FIG 4 Increased mitochondrial fragmentation in HIV- and methamphetamine-treated neurons is DRP1 dependent. (A, C, and E) Western blot analysis of mitochondrion-enriched fractions showing increased DRP1 expression with gp120, Tat, methamphetamine, and combination treatments at 24 h. NAC pretreatment abrogated DRP1-increased protein expression. (B, D, and F) Relative intensity of DRP1 protein was normalized to that of VDAC mitochondrial protein, and each data point was normalized to the results for treatment with vehicle and analyzed using ImageJ software. Student's t test was performed to test the statistical significance. Data are presented as mean values $\pm$ standard deviations ($n = 3$ independent donors). *, $P < 0.05$; **, $P < 0.01$.

microtubule-associated protein 2 (MAP2)-stained neuronal cells. HIV- and methamphetamine-treated neurons showed increased accumulation of DRP1 to the perinuclear area where damaged mitochondria are present (Fig. 5B to H). In contrast, vehicle-treated neurons (Fig. 5A) and NAC-pretreated neurons exposed to HIV and methamphetamine showed reduced expression and translocation of DRP1, suggesting that NAC efficiently prevented DRP1 upregulation (Fig. 5I to P).

Methamphetamine increases ROS production in HIV- and methamphetamine-exposed neurons. Mitochondrial dysfunction is a common mechanism of ROS production associated with many viral infections (27). HIV similarly dysregulates oxidative stress pathways by increasing ROS production and inducing mitochondrial dysfunction
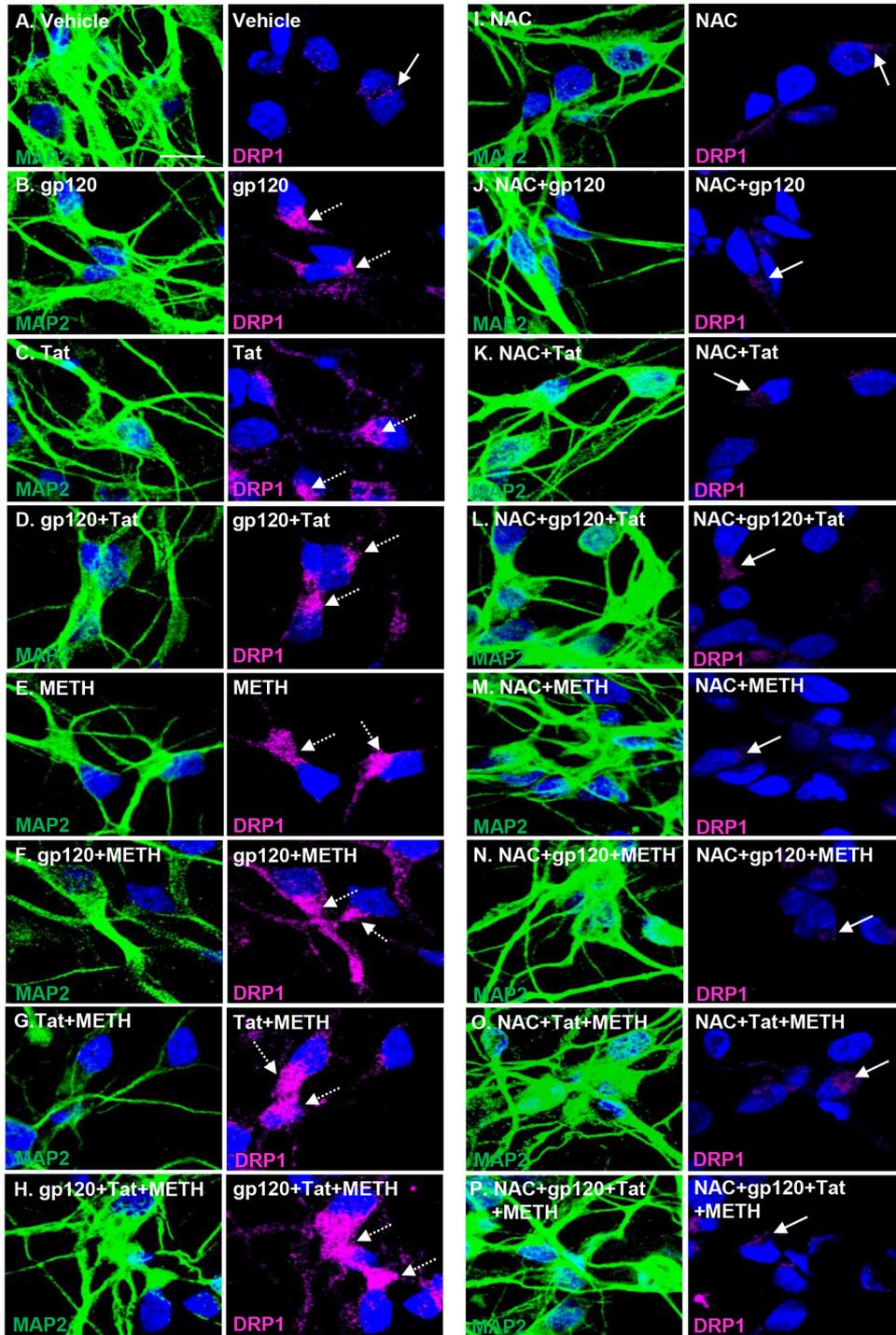
FIG 5 Methamphetamine increases mitochondrial translocation of DRP1 in HIV-treated neurons, leading to mitochondrial fission and altered mitochondrial dynamics. Neurons were immunostained with antibodies specific to DRP1 (magenta) and 4',6'-diamidino-2-phenylindole (blue) for nuclei. (A) Vehicle-treated cells display a basal level of DRP1 expression, as shown by the white arrows. (B to H) Confocal laser microscopy analysis shows increased expression and translocation of DRP1 to the perinuclear area, as shown by the white dashed arrows. (I to P) NAC pretreatment abolished DRP1 translocation, association to the mitochondria, and mitochondrial fission in HIV- and methamphetamine-treated human neuronal cells (indicated by the white arrows). Scale bar, 10 μm.

(32, 33). Increased ROS production, triggered by HIV gp120 and Tat proteins circulating in the blood, can alter the blood-brain barrier (27). We hypothesized that the increase in ROS production in neurons resulting from the mitochondrial damage triggered by HIV-specific proteins and methamphetamine in combination with HIV would increase the oxidative stress in human neurons. Oxidative stress was measured using CellROX deep red reagent, a cell-permeable dye that has bright fluorescence immediately after oxidation by ROS. CellROX magenta staining increased in each of the HIV protein- and methamphetamine-treated neurons (Fig. 6B to E) and in those with combination treatments (Fig. 6F to H), indicating an increase of ROS species. In contrast, vehicle-treated and NAC-pretreated HIV- and methamphetamine-exposed neurons showed basal levels of ROS production (Fig. 6A and I to P). Following treatment with gp120, Tat, and methamphetamine, we observed a significant corrected total cell fluorescence (CTCF) mean increase in ROS production compared to levels in the controls, with 4.1-, 4.9-, 7.2-,10.6-, 12.7-, 14.2-, and 15.9-fold increases for gp120, Tat, gp120 plus Tat (gp120/Tat), methamphetamine, methamphetamine/gp120, methamphetamine/Tat, and methamphetamine/gp120/Tat, respectively ($P < 0.05$) (Fig. 6R). These findings confirm that HIV gp120 and Tat in combination with methamphetamine increased mitochondrial dysfunction and neuronal degeneration by elevating ROS production. Pretreatment with 1 mM NAC abrogated the ROS production increase in neurons treated with HIV proteins and methamphetamine ($P =$ ns) (Fig. 6R). These results emphasize that methamphetamine further increases ROS production in HIV-treated neurons and that NAC, a ROS scavenger, has a powerful role in regulation of oxidative stress and improvement of neuronal function.

HIV in combination with methamphetamine increases neuronal degeneration. Mitochondrial dysfunction and dendritic beading are early signs of neuronal toxicity present under different pathological conditions (12). Neuronal toxicity such as synaptodendritic injury, dendritic beading, and neuronal loss are important findings in HIV-associated neuropathology (34). HIV proteins combined with cytokines and chemokines released by HIV-infected cells have been shown to induce dendritic simplification and neuronal death (35). We therefore next examined the effects of HIV proteins with and without methamphetamine by staining neurites with MAP2, a somatodendritic marker, to visualize the neuritic network. Treatment with HIV proteins, methamphetamine, and a combination of these induced qualitative changes in HPNs, manifested as dendritic beading and a reduction of dendritic complexity (Fig. 7B to H) compared to levels in vehicle-treated cells (Fig. 7A). Confocal microscopy and quantitative analyses using Fiji software revealed that the total length of neurites per cell decreased from a mean of 460 μm in vehicle-treated cells (Fig. 8A and R) to mean values of 262.6 μm, 248.8 μm, 209.4 μm, and 211.8 μm in cells treated with gp120, Tat, gp120 and Tat, and methamphetamine ($P < 0.01$ for all comparisons to control) (Fig. 8B to E and R). The combined treatment of HIV and methamphetamine further decreased the MAP2 network measured in total neurite length per cell to mean values of 179.3 μm for gp120/methamphetamine, 165.1 μm for Tat/methamphetamine, and 140 μm for gp120 and Tat/methamphetamine ($P < 0.05$ for all comparisons to controls) (Fig. 8F to H and R). Pretreatment with NAC abrogated neuronal degeneration in HIV- and methamphetamine-treated cells and maintained the length of the neuritic network at values similar to those of control cells ($P =$ ns, for all comparisons to controls) (Fig. 8I to P and R). These results show that methamphetamine in combination with HIV proteins increases neuronal toxicity and subsequently neuronal degeneration and that NAC pretreatment abrogates the MAP2 network damage in human neurons.

NAC posttreatment reverses mitochondrial morphological changes and reduces ROS levels in HIV-treated neurons. High ROS levels play a central role in mitochondrial fragmentation. To assess the effect of NAC on the recovery of neuronal mitochondria after HIV protein and methamphetamine exposure, neurons were treated to HIV proteins and/or methamphetamine for 24 h, followed by treatment with NAC for 48 h (Fig. 9A to P). Quantification of mitochondrial lengths in neurons treated with vehicle, HIV proteins, and methamphetamine for 24 h (Fig. 9A to H and R) revealed a
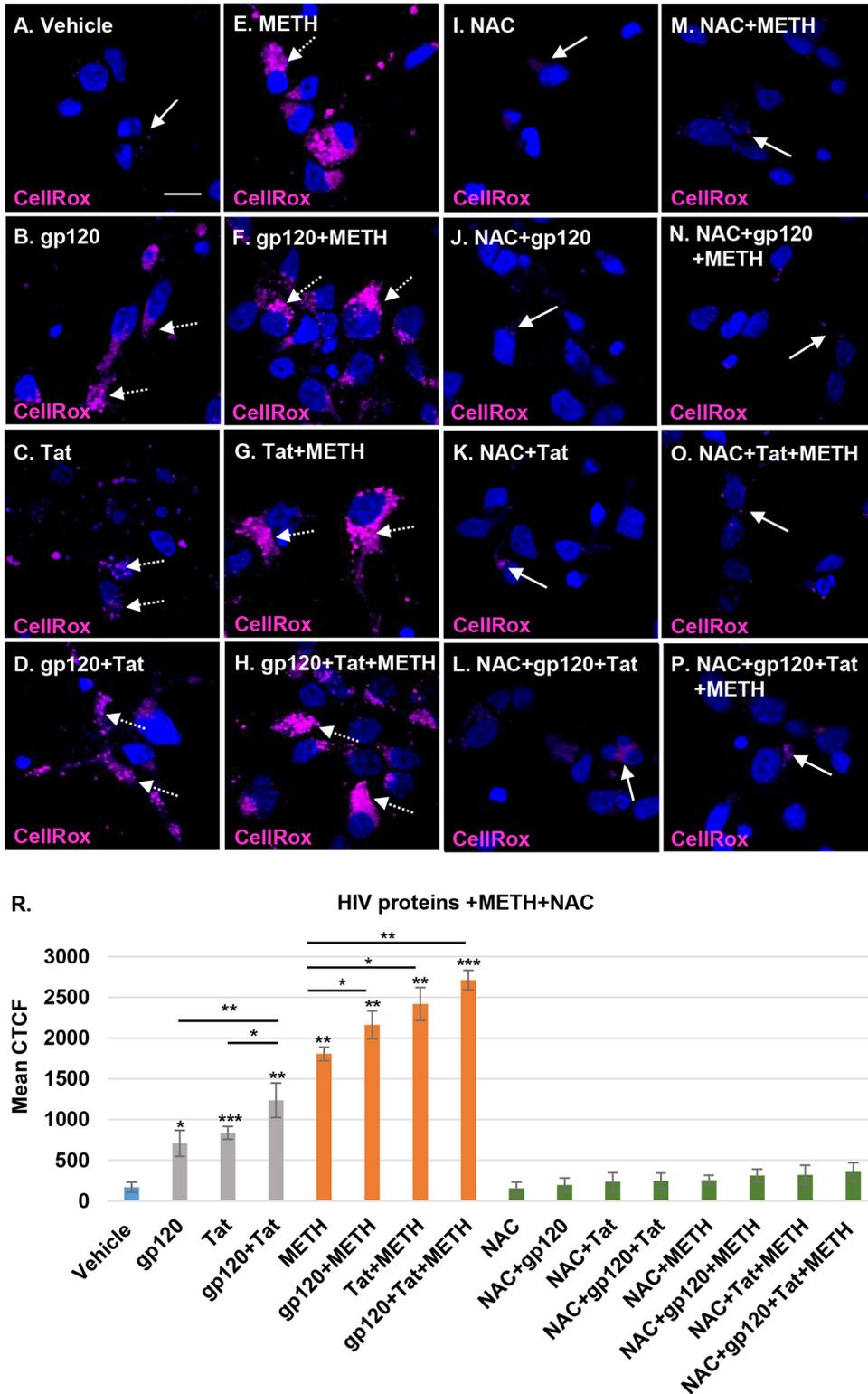
FIG 6 Methamphetamine increases mitochondrial dysfunction and damage in HIV-treated neurons by elevating ROS production. (A to H) Neurons were treated with HIV proteins alone, methamphetamine alone, or combinations of these. The cells were treated with 5 μM CellROX deep red reagent for 30 min before fixation. Nuclei were stained with 4′,6′-diamidino-2-phenylindole (blue). (I to P) NAC pretreatment of HIV- and methamphetamine-treated cells. (R) Confocal microscopy and ImageJ were used to measure the mean of the CTCF for the CellROX staining in treated cells. Student's t test was performed to test the statistical significance. Data are presented as mean values $\pm$ standard deviations ($n = 3$ independent donors). *, $P < 0.05$; **, $P < 0.01$; ***, $P < 0.001$. Scale bar, 10 μm.
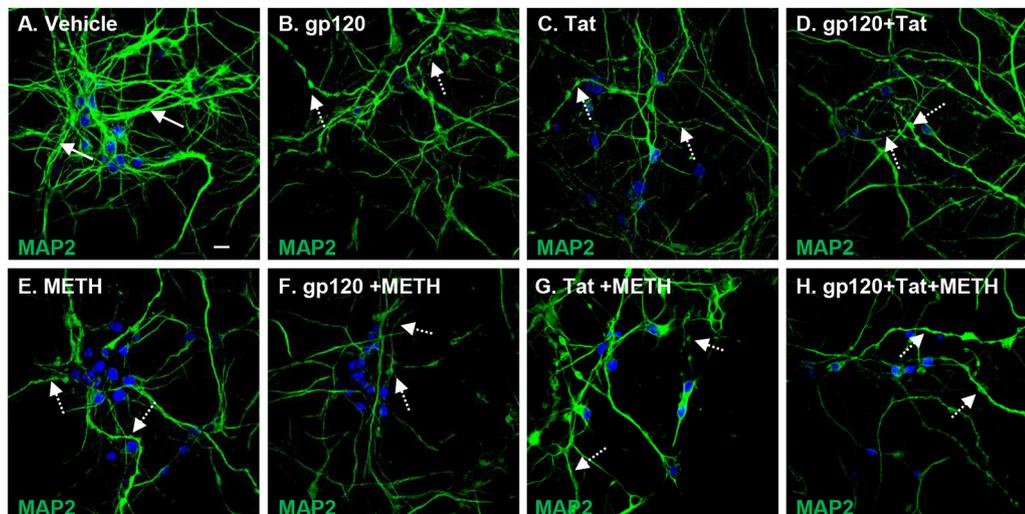
FIG 7 Methamphetamine increases neuronal toxicity in HIV-treated human primary neurons. MAP2 antibody was used for staining neuronal dendrites. (A) Confocal laser microscopy showing a healthy MAP2 dendritic network (as indicated by the white arrows). (B to H) HIV, methamphetamine, and combination treatments induced dendritic beading and dendritic size reduction (as indicated by the white dashed arrows). Scale bar, 10 μm.

pattern of mitochondrial fragmentation similar to that shown in Fig. 3. Treatment with NAC following exposure to HIV and methamphetamine (Fig. 9I to P and R) completely reversed mitochondrial fragmentation, suggesting that elevated neurotoxic levels of ROS can be reversed when ROS levels are decreased. To further confirm this finding, we monitored ROS levels by measuring oxidative stress as described in the legend of Fig. 6. HIV gp120, HIV Tat, methamphetamine, and combination treatments of gp120 plus methamphetamine, Tat plus methamphetamine, and gp120 plus Tat plus methamphetamine showed an increase in levels of CellROX magenta staining and a significant CTCF mean increase in ROS production levels of 3.2-,4.5-, 8.9-, 9.6-, 11.5-, 14.2-, and 16.3-fold compared to levels for controls ($P < 0.05$) (Fig. 10B to H and R). Posttreatment with NAC significantly decreased ROS production to levels similar to those of vehicle-treated cells ($P = $ ns) (Fig. 10I to P and R). These findings reinforce that elevated ROS production is involved in mitochondrial fragmentation and that NAC treatment can reverse the pathological effects of HIV and methamphetamine in neurons.

DISCUSSION

The pathogenesis of HIV-associated neurocognitive disorders in the ART era is multifactorial, with viral, antiretroviral, inflammatory, genetic, and environmental factors potentially contributing to the development and persistence of CNS impairment. The use of drugs of abuse, including methamphetamine, is common among PLWH and can alter the CNS effects of HIV (36). Methamphetamine has been associated with neurotoxicity, blood-brain barrier damage, neurodegeneration, and impairment of cognitive function (15, 37, 38). The methamphetamine effects on the brain neurochemistry and function are due to the high distribution and retention of this lipid-soluble molecule in high-lipid-content tissues like the brain (20). In binge users, the brain-to-serum concentration can reach a ratio of 13:1, which is the equivalent of 200 to 1,040 μM methamphetamine accumulated in the brain (20, 21). Additionally, methamphetamine use has been associated with increased risk for HIV transmission, immune dysfunction, and accelerated HIV/AIDS disease progression (39). Animal and human studies have shown that methamphetamine in combination with HIV increases neuronal injury and oxidative stress in the brain (36, 40). Additionally, *in vivo* studies have identified increased synaptodendritic damage, astrogliosis and microgliosis, and neurobehavioral changes in HIV gp120 and Tat transgenic mice treated with methamphetamine (36, 41).
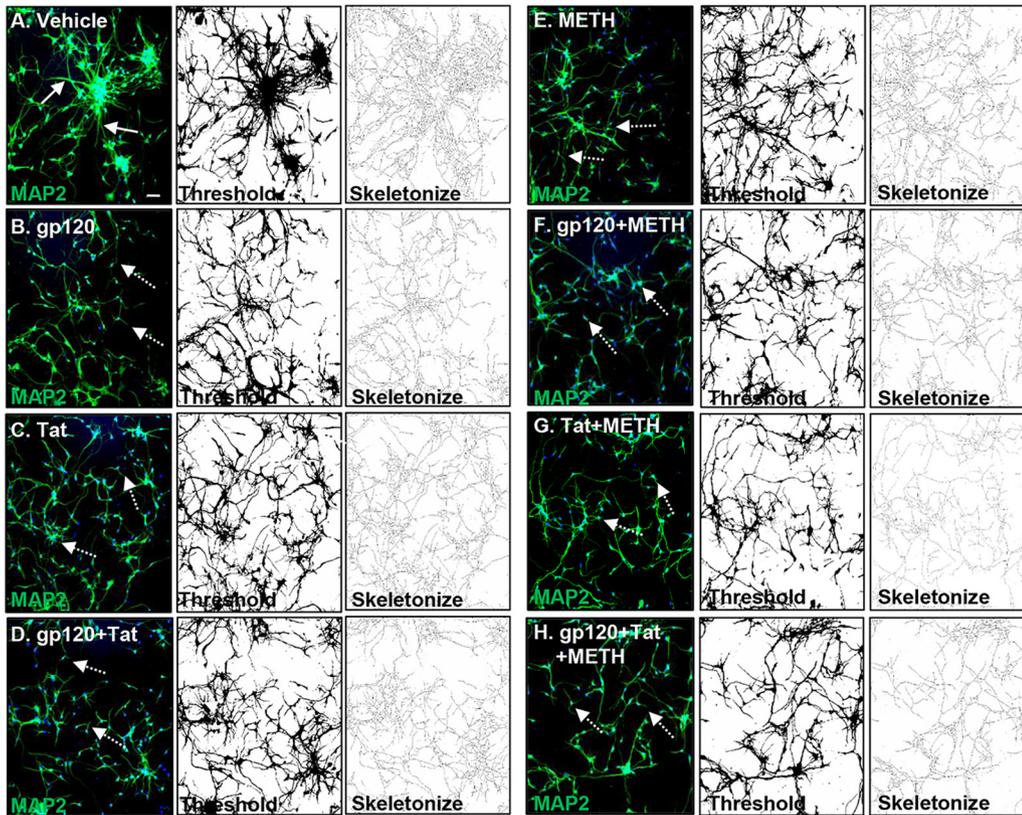
FIG 8 Quantitative analysis of MAP2 dendritic network. (A) Confocal analysis shows that vehicle-treated cells display a healthy neuronal network (as indicated by the white arrows). (B to H) Confocal analysis of MAP2 dendritic network showing a reduction of the neuronal dendrites in HIV, methamphetamine, or combination treatments (as indicated by the white dashed arrows). (I to P) NAC pretreatment abrogated dendritic reduction in HIV- and methamphetamine-treated neurons (indicated by the white arrows). For panels A to P and panel R, Fiji software analysis was used to process and analyze confocal images by applying thresholding and skeletonization functions. The Simple Neurite Tracer function was used to quantify the length of the neuronal dendrites. Student's t test was performed to test the statistical significance. Data are presented as mean values ± standard deviations ($n = 3$ independent donors). *, $P < 0.05$; **, $P < 0.01$; ***, $P < 0.001$. Scale bar, 50 μm.

Previously, we showed that in human neurons HIV proteins alter mitochondrial dynamics, induce incomplete mitophagy, and block the clearance of damaged mitochondria. Here, we report that methamphetamine potentiates the effects of HIV proteins on mitochondrial damage in human neurons. Our findings show that methamphetamine exposure of neurons in combination with HIV increases LC3B-II lipidation, blocks autophagic flux, and inhibits the elimination of damaged mitochondria. Combined exposure to HIV and methamphetamine increased DRP1-dependent mitochondrial fragmentation and p62 translocation and aggregation to damaged mitochondria, indicating impairment of mitochondrial turnover. Methamphetamine and HIV also increased neuronal oxidative stress by increasing ROS production, resulting in alteration of the neuronal network as determined by the reduction in neurite length.

Previous studies have shown that modifications in mitochondrial morphology and function are correlated with ROS induction. NAC (a ROS scavenger) reduced ROS production, and methamphetamine induced hyperthermia in mice (42, 43). Studies in *Drosophila* pinpointed the importance of ROS for mitochondrial and tissue dynamics and for ROS-induced mitochondrial fragmentation. Conversely, suppressing ROS resulted in a transition to tubular mitochondrial morphology (43, 44). In cells, mitochondrial dynamics are mediated by dynamin-related GTPases like mitofusin 1 (MFN1) and MFN2 for fusion and DRP1 for fission or fragmentation (45, 46). Other antioxidants like Trolox have been reported to increase glutathione-and mitofusin-dependent mitochondrial filamentation (47). Neurons are sensitive to ROS-mediated damage, and ROS
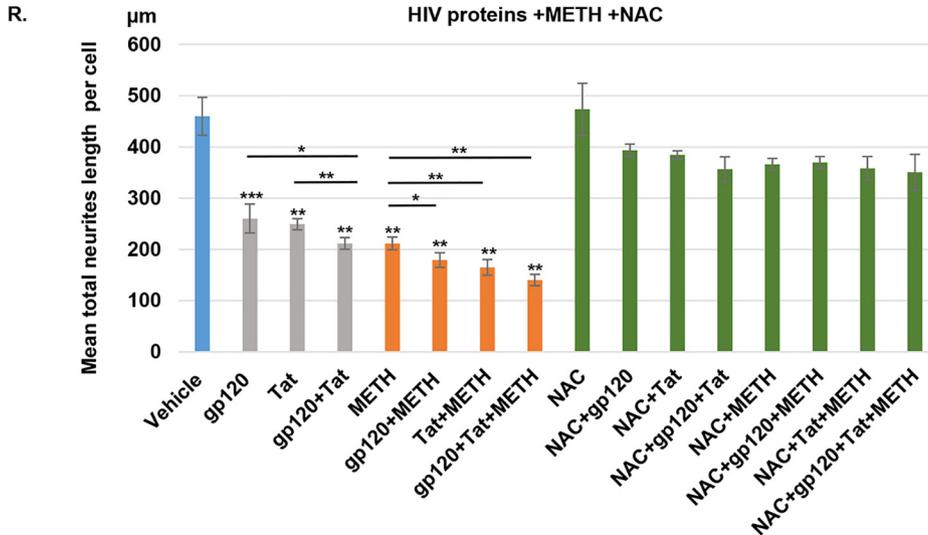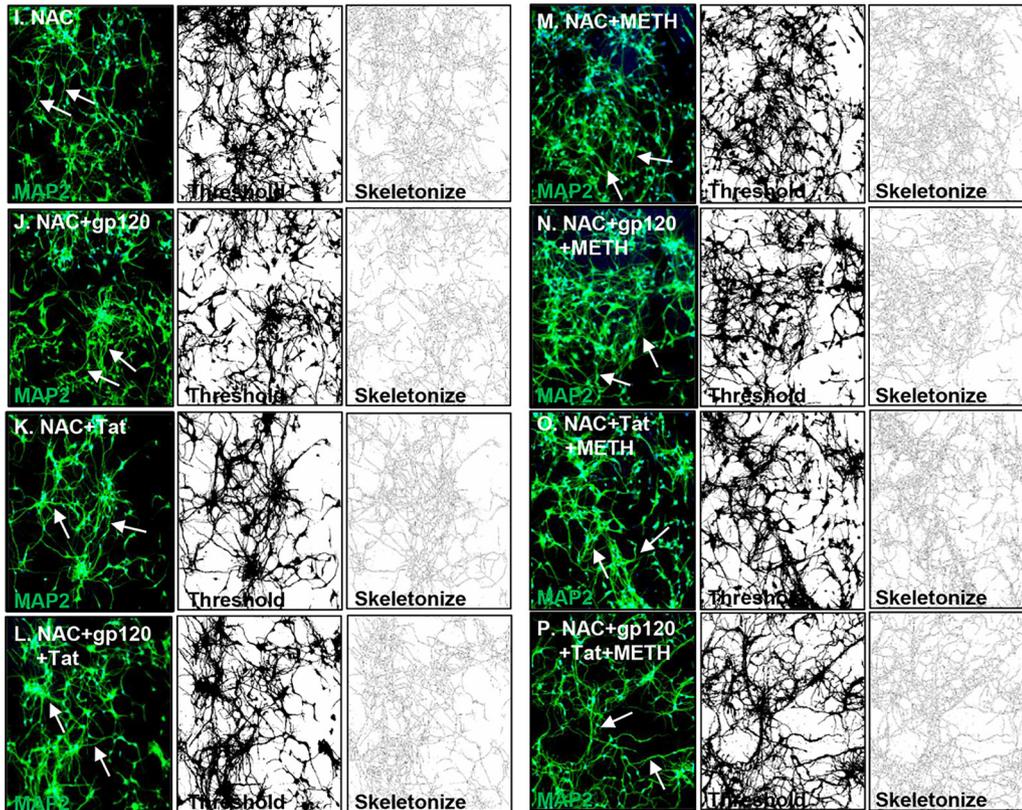
FIG 8 (Continued)

exposure induces changes in the calcium homeostasis, mitochondrial dysfunction, and microtubule destabilization along with the appearance of neurite beading and neurite degeneration (48). Treatment with antioxidants like vitamin E has been shown to prevent neuronal degeneration (48).

The importance of oxidative stress in driving the pathogenesis of HIV/methamphetamine-driven neurotoxicity is further supported by the beneficial effects of the antioxidant NAC. Both pre- and posttreatment with NAC abrogated HIV/methamphetamine-induced mitochondrial and neuronal toxicity, as determined by the prevention of MAP2 neurite length reduction, DRP1-mediated mitochondrial frag-
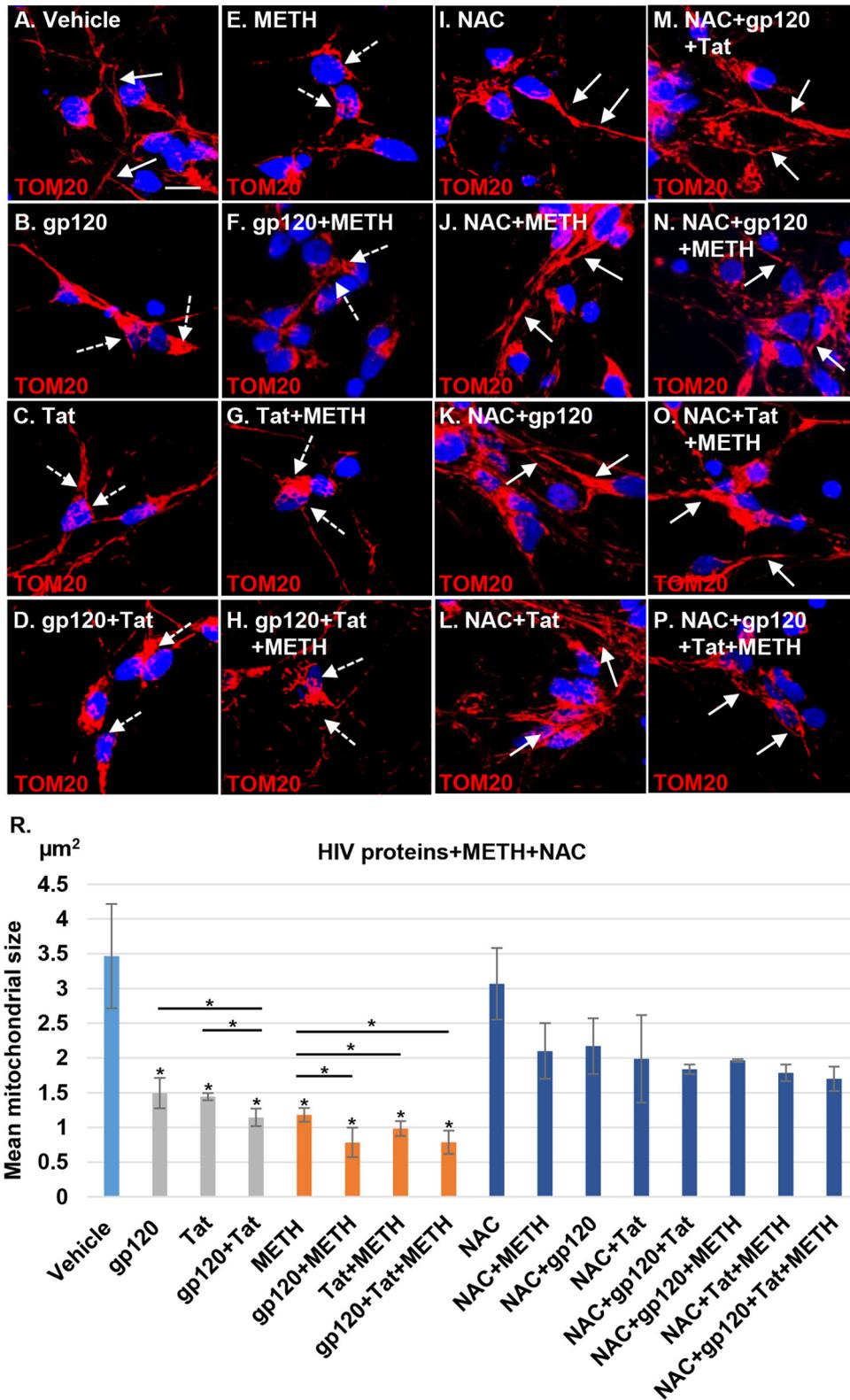
FIG 9 Mitochondrial shape and network disruption are reversed by NAC posttreatment in HIV-treated cells. (A) Confocal laser microscopy analysis showing healthy tubular mitochondrial structures (indicated by the white arrows) in vehicle-treated cells. (B to H) Cells were treated for 24 h with 100 ng/ml gp120, Tat, or gp120/Tat and 300 μM methamphetamine alone or in combination with HIV proteins. Confocal microscopy shows mitochondrial aggregation and fragmentation (indicated by the dashed white arrows). Mitochondria were stained with TOM20 (red); 4′,6′-diamidino-2-phenylindole (blue) was used to stain nuclei. (I to P) HIV- and methamphetamine-exposed neurons after treatment for 48 h with NAC. Confocal microscopy shows the recovery of the mitochondrial size

(Continued on next page)

mentation, and increased ROS production. NAC, a glutathione precursor, is an old drug with neuroprotective properties that has been used to treat a number of psychiatric and neurological conditions (49, 50). NAC is able to cross the blood-brain barrier and directly improve mitochondrial and neuronal function when oxidative stress is present (51, 52).

The present study suggests that ROS production is involved in mitochondrial fragmentation and neuronal degeneration in HIV- and methamphetamine-treated human neurons and that NAC prevented and reversed these harmful neuronal effects. We do not exclude the potential role of NAC in the regulation of mitochondrial dynamics by decreasing ROS production and DRP1 levels in human neurons. Mitochondria can adopt a variety of shapes depending on the cell type and metabolic state. However, despite the recent progress in live-cell microscopy, it is still unclear how mitochondrial morphology affects mitochondrial function (46). Since redox homeostasis and mitochondrial morphology are interrelated, antioxidants have been reported to stimulate MFN2-dependent mitochondrial filamentation (44, 53), reinforcing the potential role of NAC in regulating mitochondrial morphology.

Mitochondrial health is critical to the function of neurons, whereas mitochondrial dysfunction and aberrant mitophagy have been associated with a wide range of neurodegenerative diseases and premature aging (54). Exposure of neurons to HIV Tat has been associated with altered mitochondrial oxidative phosphorylation (OXPHOS) enzyme activity and impaired neuronal synaptic function. Moreover, recent studies have identified that HIV is associated with mitochondrial changes that affect brain structure independent of ART or age (55). The association of impaired mitophagy in the presence of HIV proteins that is increased by the presence of methamphetamine suggests that the combination may also be associated with the accelerated aging observed in HIV-infected persons receiving ART.

Our findings have potential therapeutic implications for PLWH with neurocognitive impairment and methamphetamine use (56). Although the goal should be to counsel PLWH to reduce their substance use, targeting mitochondria by controlling ROS production through intracellular delivery of an antioxidant such as NAC could control the progression of mitochondrial dysfunction and CNS impairment in this group of patients (57). In this regard, NAC has been shown to have beneficial effects on HIV infection in chronic and acute experimental infection models (50, 58) and, thus, further supports clinical trials to examine the benefits of such treatment.

In summary, we have determined that the combination of HIV gp120 or Tat with methamphetamine increases mitochondrial DRP1-dependent fragmentation and neuronal degeneration with inhibition of mitophagy. We further demonstrate that NAC, an antioxidant and ROS scavenger, is able to prevent and treat these effects in neurons, suggesting a potential therapeutic target to reduce ROS and the effects of HIV and methamphetamine on the CNS.

MATERIALS AND METHODS

Chemical reagents and antibodies. Chemicals used were (+)-methamphetamine hydrochloride (Millipore Sigma), bafilomycin A1 (Enzo Life Sciences), and CellROX deep red reagent (Thermo Fisher Scientific). Primary antibodies used included the following: rabbit monoclonal anti-DRP1 (Novus Biologicals), rabbit monoclonal anti-voltage-dependent anion channel protein (VDAC) (Cell Signaling), mouse monoclonal anti-SQSTM1/p62 (Abcam), mouse monoclonal anti-TOM20 (BD Biosciences, Santa Cruz Biotechnologies), rabbit polyclonal anti-TOM20 (Santa Cruz Biotechnology), mouse monoclonal anti-actin (Millipore Sigma), and chicken monoclonal anti-MAP2 (Novus Biologicals). Secondary antibodies used for immunofluorescence experiments were Alexa Fluor 488, 568, and 647 donkey and goat anti-mouse, anti-rabbit, and anti-chicken IgG (Invitrogen). HIV-1 IIIB gp120 (no. 11784) and HIV-1 IIIB Tat (no. 2222) recombinant proteins were obtained from the NIH AIDS Reagent Program. The HIV protein concentrations used are consistent with the concentrations used in other studies in which the physiological roles

FIG 9 Legend (Continued)
following NAC posttreatment. (R) Quantitative analysis of mitochondrial size using ImageJ-Fiji software. Student's t test was performed to test the statistical significance. Data are presented as mean values $\pm$ standard deviations ($n = 3$ independent donors). *, $P < 0.05$. Scale bar, 10 μm.
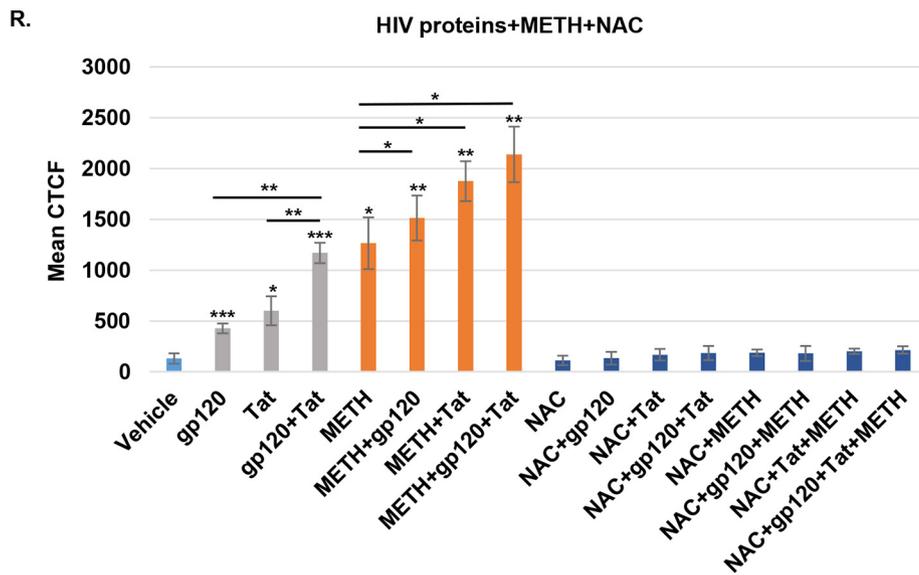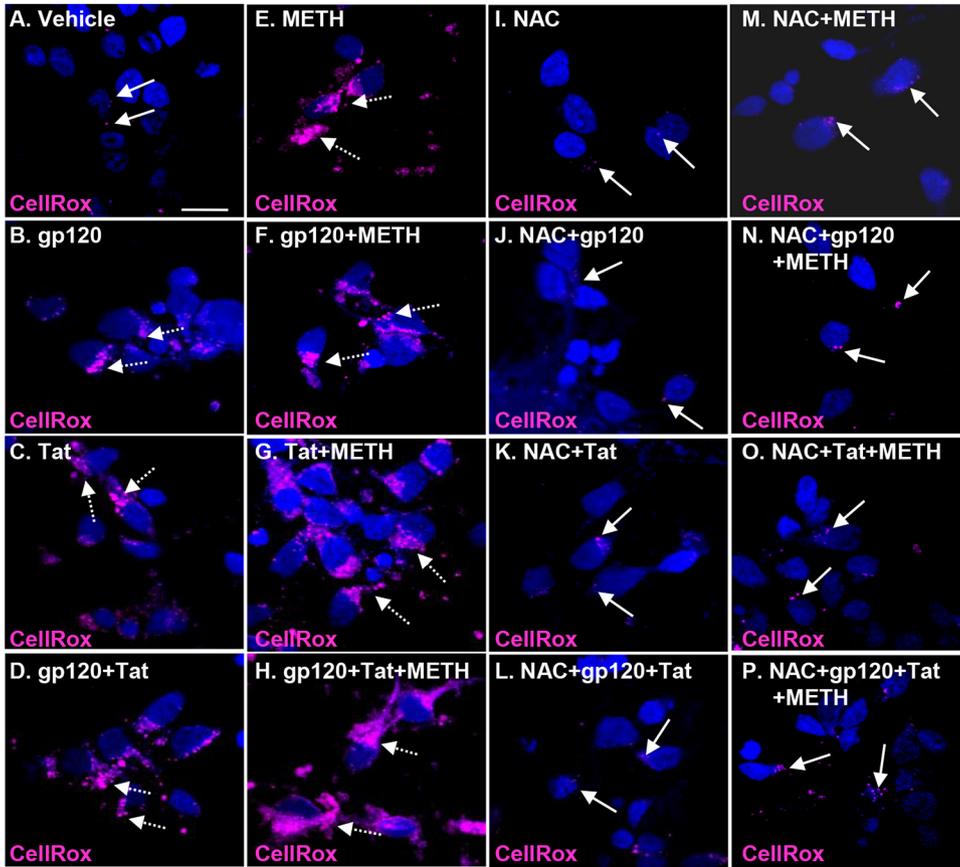
FIG 10 Increased ROS production is abrogated by NAC posttreatment in HIV-treated neuronal cells. (A to H) Neurons were treated with vehicle, HIV proteins alone, methamphetamine alone, or combinations, followed by 48 h of NAC posttreatment (I to P). Cells were treated with 5 μM CellROX deep red reagent for 30 min before fixation. Nuclei were stained with 4′,6′-diamidino-2-phenylindole (blue). (R) Confocal microscopy and ImageJ were used to measure the mean of the CTCF for the CellROX staining in treated cells. Student's t test was performed to test the statistical significance. Data are presented as mean values ± standard deviations ($n = 3$ independent donors). *, $P < 0.05$; **, $P < 0.01$; ***, $P < 0.001$. Scale bar, 10 μm.

of HIV gp120 and Tat were examined in tissues where the localized concentration is expected to be greater than that detected in serum from HIV-infected individuals (7, 25, 59–63). The NAC concentration used is consistent with the concentrations used in other neuronal studies showing that 1 mM NAC has a neuroprotective effect and does not significantly increase cell toxicity (64–69).

Cell culture, immunofluorescence, and imaging. To isolate human primary neurons (HPNs) we used forebrain fetal tissue (90 to 130 days of gestation) obtained from Advanced Bioscience Resources (Alameda, CA) and from the University of Washington, School of Medicine (Seattle, WA), according to the University of California San Diego Institutional Review Board guidelines, and processed as previously described (10, 70, 71). After 2 weeks in culture, isolated human neurons are fully differentiated and have functional synapses similar to those of mature neurons (10, 70, 72). Neurons were seeded at 10^5 cells per well on poly-D-lysine/laminin-coated glass coverslips (Corning) in 24-well plates and kept in neurobasal medium (Gibco) supplemented with B-27 (Gibco), 2 mM GlutaMAX (Gibco), and 10 μg/ml gentamicin (Gibco) for 2 weeks, with a change of medium every 3 days (71). For immunostaining experiments, a 4% paraformaldehyde (PFA) solution (Electron Microscopy Sciences) with sucrose in phosphate-buffered saline (PBS) was used for cell fixation, and 0.25% Triton X-100 solution in PBS was used to perform cell permeabilization (71). Cells were incubated with the specific primary antibodies, followed by Alexa Fluor-conjugated secondary antibodies. Microscopic images were obtained using Olympus FluoView FV1000 confocal microscopy and minimally processed using Adobe Photoshop. Mitochondrial size quantification was performed using Fiji-ImageJ software. For neurite size quantification, Simple Neurite Tracer (Fiji-ImageJ) software was used.

Western blot analysis. For immunoblotting experiments, neurons were seeded at 5×10^5 per well in poly-D-lysine/laminin-coated six-well dishes (Corning) and maintained as described above. A mitochondrion isolation kit for cultured cells (Thermo Fisher Scientific) was used to prepare mitochondrion-enriched fractions according to the supplier's instructions. Extracted cell lysates were clarified by centrifugation, subjected to SDS-PAGE, and then transferred to nitrocellulose (NC) membranes or polyvinylidene difluoride (PVDF) membranes using a Bolt Western blotting system (Thermo Fisher Scientific). Membranes were blocked with 5% bovine serum albumin (BSA; Sigma-Aldrich) in PBS supplemented with 0.1% Tween 20 (Sigma-Aldrich) and incubated with primary antibodies, followed by detection with a Western Breeze immunodetection kit (Thermo Fisher Scientific).

ROS detection assay. CellROX oxidative stress reagents were used to measure reactive oxygen species (ROS) in fixed cells according to the manufacturer's protocol. ImageJ/Fiji was used to measure corrected total cell fluorescence (CTCF). CTCF was calculated using the following formula: CTCF = integrated density $-$(area of selected cell $\times$ mean fluorescence of background readings). To calculate the final average fluorescence intensity value, CTCF was divided by the total number of cells.

Analysis. Paired Student's t tests were used to analyze the statistical significance for all data. A P value of <0.05 were considered statistically significant.

Ethics statement. The use of normal human fetal brain was approved by the Human Research Protection Program of the University of California, San Diego (project no. 150172XX; IRB exempt), in accordance with the requirements of the Code of Federal Regulation on the Protection of Human subjects [45 CFR§46.102 (f)].

represent the official views of the NIH. The funders had no role in study design, data collection and analysis, the decision to publish, or preparation of the manuscript.

We have no competing financial interests to declare.

REFERENCES

1. Saylor D, Dickens AM, Sacktor N, Haughey N, Slusher B, Pletnikov M, Mankowski JL, Brown A, Volsky DJ, McArthur JC. 2016. HIV-associated neurocognitive disorder—pathogenesis and prospects for treatment. Nat Rev Neurol 12:234–248. https://doi.org/10.1038/nrneurol.2016.27.
2. Spudich S, Gonzalez-Scarano F. 2012. HIV-1-related central nervous system disease: current issues in pathogenesis, diagnosis, and treatment. Cold Spring Harb Perspect Med 2:a007120. https://doi.org/10.1101/cshperspect.a007120.
3. Heaton RK, Clifford DB, Franklin DR, Jr, Woods SP, Ake C, Vaida F, Ellis RJ, Letendre SL, Marcotte TD, Atkinson JH, Rivera-Mindt M, Vigil OR, Taylor MJ, Collier AC, Marra CM, Gelman BB, McArthur JC, Morgello S, Simpson DM, McCutchan JA, Abramson I, Gamst A, Fennema-Notestine C, Jernigan TL, Wong J, Grant I, Group C, CHARTER Group. 2010. HIV-associated neurocognitive disorders persist in the era of potent antiretroviral therapy: CHARTER Study. Neurology 75:2087–2096. https://doi.org/10.1212/WNL.0b013e318200d727.
4. Sanchez AB, Kaul M. 2017. Neuronal stress and injury caused by HIV-1, cART and drug abuse: converging contributions to HAND. Brain Sci 7:25. https://doi.org/10.3390/brainsci7030025.
5. Klionsky DJ. 2005. The molecular machinery of autophagy: unanswered questions. J Cell Sci 118:7–18. https://doi.org/10.1242/jcs.01620.
6. Alirezaei M, Kiosses WB, Fox HS. 2008. Decreased neuronal autophagy in HIV dementia: a mechanism of indirect neurotoxicity. Autophagy 4:963–966. https://doi.org/10.4161/auto.6805.
7. Fields J, Dumaop W, Eleuteri S, Elueteri S, Campos S, Serger E, Trejo M, Kosberg K, Adame A, Spencer B, Rockenstein E, He JJ, Masliah E. 2015. HIV-1 Tat alters neuronal autophagy by modulating autophagosome fusion to the lysosome: implications for HIV-associated neurocognitive disorders. J Neurosci 35:1921–1938. https://doi.org/10.1523/JNEUROSCI.3207-14.2015.
8. Spector SA, Zhou D. 2008. Autophagy: an overlooked mechanism of HIV-1 pathogenesis and neuroAIDS? Autophagy 4:704–706. https://doi.org/10.4161/auto.6105.
9. Ojha CR, Lapierre J, Rodriguez M, Dever SM, Zadeh MA, DeMarino C, Pleet ML, Kashanchi F, El-Hage N. 2017. Interplay between autophagy, exosomes and HIV-1 associated neurological disorders: new insights for diagnosis and therapeutic applications. Viruses 9:176. https://doi.org/10.3390/v9070176.
10. Teodorof-Diedrich C, Spector SA. 2018. Human immunodeficiency virus type 1 gp120 and Tat induce mitochondrial fragmentation and incomplete mitophagy in human neurons. J Virol 92:e00993-18. https://doi.org/10.1128/JVI.00993-18.
11. Martinez-Vicente M. 2017. Neuronal mitophagy in neurodegenerative diseases. Front Mol Neurosci 10:64. https://doi.org/10.3389/fnmol.2017.00064.
12. Greenwood SM, Mizielinska SM, Frenguelli BG, Harvey J, Connolly CN. 2007. Mitochondrial dysfunction and dendritic beading during neuronal toxicity. J Biol Chem 282:26235–26244. https://doi.org/10.1074/jbc.M704488200.
13. Cotto B, Natarajanseenivasan K, Langford D. 2019. HIV-1 infection alters energy metabolism in the brain: contributions to HIV-associated neurocognitive disorders. Prog Neurobiol 181:101616. https://doi.org/10.1016/j.pneurobio.2019.101616.
14. Var SR, Day TR, Vitomirov A, Smith DM, Soontornniyomkij V, Moore DJ, Achim CL, Mehta SR, Perez-Santiago J. 2016. Mitochondrial injury and cognitive function in HIV infection and methamphetamine use. AIDS 30:839–848. https://doi.org/10.1097/QAD.0000000000001027.
15. Tian C, Murrin LC, Zheng JC. 2009. Mitochondrial fragmentation is involved in methamphetamine-induced cell death in rat hippocampal neural progenitor cells. PLoS One 4:e5546. https://doi.org/10.1371/journal.pone.0005546.
16. Cao L, Fu M, Kumar S, Kumar A. 2016. Methamphetamine potentiates HIV-1 gp120-mediated autophagy via Beclin-1 and Atg5/7 as a pro-survival response in astrocytes. Cell Death Dis 7:e2425. https://doi.org/10.1038/cddis.2016.317.
17. Hoefer MM, Sanchez AB, Maung R, de Rozieres CM, Catalan IC, Dowling CC, Thaney VE, Pina-Crespo J, Zhang D, Roberts AJ, Kaul M. 2015.

Combination of methamphetamine and HIV-1 gp120 causes distinct long-term alterations of behavior, gene expression, and injury in the central nervous system. Exp Neurol 263:221–234. https://doi.org/10.1016/j.expneurol.2014.09.010.
18. Dikic I, Elazar Z. 2018. Mechanism and medical implications of mammalian autophagy. Nat Rev Mol Cell Biol 19:349–364. https://doi.org/10.1038/s41580-018-0003-4.
19. Cuervo AM. 2004. Autophagy: in sickness and in health. Trends Cell Biol 14:70–77. https://doi.org/10.1016/j.tcb.2003.12.002.
20. Riviere GJ, Gentry WB, Owens SM. 2000. Disposition of methamphetamine and its metabolite amphetamine in brain and other tissues in rats after intravenous administration. J Pharmacol Exp Ther 292:1042–1047.
21. Melega WP, Cho AK, Harvey D, Lacan G. 2007. Methamphetamine blood concentrations in human abusers: application to pharmacokinetic modeling. Synapse 61:216–220. https://doi.org/10.1002/syn.20365.
22. Thangaraj A, Periyasamy P, Liao K, Bendi VS, Callen S, Pendyala G, Buch S. 2018. HIV-1 TAT-mediated microglial activation: role of mitochondrial dysfunction and defective mitophagy. Autophagy 14:1596–1619. https://doi.org/10.1080/15548627.2018.1476810.
23. Avdoshina V, Fields JA, Castellano P, Dedoni S, Palchik G, Trejo M, Adame A, Rockenstein E, Eugenin E, Masliah E, Mocchetti I. 2016. The HIV protein gp120 alters mitochondrial dynamics in neurons. Neurotox Res 29:583–593. https://doi.org/10.1007/s12640-016-9608-6.
24. Fields JA, Serger E, Campos S, Divakaruni AS, Kim C, Smith K, Trejo M, Adame A, Spencer B, Rockenstein E, Murphy AN, Ellis RJ, Letendre S, Grant I, Masliah E. 2016. HIV alters neuronal mitochondrial fission/fusion in the brain during HIV-associated neurocognitive disorders. Neurobiol Dis 86:154–169. https://doi.org/10.1016/j.nbd.2015.11.015.
25. Rozzi SJ, Avdoshina V, Fields JA, Mocchetti I. 2018. Human immunodeficiency virus Tat impairs mitochondrial fission in neurons. Cell Death Discov 4:8. https://doi.org/10.1038/s41420-017-0013-6.
26. Knott AB, Perkins G, Schwarzenbacher R, Bossy-Wetzel E. 2008. Mitochondrial fragmentation in neurodegeneration. Nat Rev Neurosci 9:505–518. https://doi.org/10.1038/nrn2417.
27. Ivanov AV, Valuev-Elliston VT, Ivanova ON, Kochetkov SN, Starodubova ES, Bartosch B, Isaguliants MG. 2016. Oxidative Stress during HIV Infection: mechanisms and Consequences. Oxid Med Cell Longev 2016:8910396. https://doi.org/10.1155/2016/8910396.
28. Visalli V, Muscoli C, Sacco I, Sculco F, Palma E, Costa N, Colica C, Rotiroti D, Mollace V. 2007. N-acetylcysteine prevents HIV gp 120-related damage of human cultured astrocytes: correlation with glutamine synthase dysfunction. BMC Neurosci 8:106. https://doi.org/10.1186/1471-2202-8-106.
29. Vantaggiato C, Castelli M, Giovarelli M, Orso G, Bassi MT, Clementi E, De Palma C. 2019. The fine tuning of Drp1-dependent mitochondrial remodeling and autophagy controls neuronal differentiation. Front Cell Neurosci 13:120. https://doi.org/10.3389/fncel.2019.00120.
30. Reddy PH, Reddy TP, Manczak M, Calkins MJ, Shirendeb U, Mao P. 2011. Dynamin-related protein 1 and mitochondrial fragmentation in neurodegenerative diseases. Brain Res Rev 67:103–118. https://doi.org/10.1016/j.brainresrev.2010.11.004.
31. Chan DC. 2012. Fusion and fission: interlinked processes critical for mitochondrial health. Annu Rev Genet 46:265–287. https://doi.org/10.1146/annurev-genet-110410-132529.
32. Banki K, Hutter E, Gonchoroff NJ, Perl A. 1998. Molecular ordering in HIV-induced apoptosis. Oxidative stress, activation of caspases, and cell survival are regulated by transaldolase. J Biol Chem 273:11944–11953. https://doi.org/10.1074/jbc.273.19.11944.
33. Deshmane SL, Mukerjee R, Fan S, Del Valle L, Michiels C, Sweet T, Rom I, Khalili K, Rappaport J, Amini S, Sawaya BE. 2009. Activation of the oxidative stress pathway by HIV-1 Vpr leads to induction of hypoxia-inducible factor 1α expression. J Biol Chem 284:11364–11373. https://doi.org/10.1074/jbc.M809266200.
34. Ellis R, Langford D, Masliah E. 2007. HIV and antiretroviral therapy in the brain: neuronal injury and repair. Nat Rev Neurosci 8:33–44. https://doi.org/10.1038/nrn2040.
35. Mocchetti I, Bachis A, Avdoshina V. 2012. Neurotoxicity of human im-

munodeficiency virus-1: viral proteins and axonal transport. Neurotox Res 21:79–89. https://doi.org/10.1007/s12640-011-9279-2.

36. Soontornniyomkij V, Kesby JP, Morgan EE, Bischoff-Grethe A, Minassian A, Brown GG, Grant I, Translational Methamphetamine ARCG. 2016. Effects of HIV and methamphetamine on brain and behavior: evidence from human studies and animal models. J Neuroimmune Pharmacol 11:495–510. https://doi.org/10.1007/s11481-016-9699-0.

37. Rusyniak DE. 2011. Neurologic manifestations of chronic methamphetamine abuse. Neurol Clin 29:641–655. https://doi.org/10.1016/j.ncl.2011.05.004.

38. Northrop NA, Yamamoto BK. 2015. Methamphetamine effects on blood-brain barrier structure and function. Front Neurosci 9:69. https://doi.org/10.3389/fnins.2015.00069.

39. Passaro RC, Pandhare J, Qian HZ, Dash C. 2015. The complex interaction between methamphetamine abuse and HIV-1 pathogenesis. J Neuroimmune Pharmacol 10:477–486. https://doi.org/10.1007/s11481-015-9604-2.

40. Jang EY, Yang CH, Hedges DM, Kim SP, Lee JY, Ekins TG, Garcia BT, Kim HY, Nelson AC, Kim NJ, Steffensen SC. 2017. The role of reactive oxygen species in methamphetamine self-administration and dopamine release in the nucleus accumbens. Addict Biol 22:1304–1315. https://doi.org/10.1111/adb.12419.

41. Crews L, Lentz MR, Gonzalez RG, Fox HS, Masliah E. 2008. Neuronal injury in simian immunodeficiency virus and other animal models of neuroAIDS. J Neurovirol 14:327–339. https://doi.org/10.1080/13550280802132840.

42. Sanchez-Alavez M, Conti B, Wood MR, Bortell N, Bustamante E, Saez E, Fox HS, Marcondes MC. 2013. ROS and sympathetically mediated mitochondria activation in brown adipose tissue contribute to methamphetamine-induced hyperthermia. Front Endocrinol (Lausanne) 4:44. https://doi.org/10.3389/fendo.2013.00044.

43. Sanchez-Alavez M, Bortell N, Galmozzi A, Conti B, Marcondes MC. 2014. Reactive oxygen species scavenger N-acetyl cysteine reduces methamphetamine-induced hyperthermia without affecting motor activity in mice. Temperature (Austin) 1:227–241. https://doi.org/10.4161/23328940.2014.984556.

44. Muliyil S, Narasimha M. 2014. Mitochondrial ROS regulates cytoskeletal and mitochondrial remodeling to tune cell and tissue dynamics in a model for wound healing. Dev Cell 28:239–252. https://doi.org/10.1016/j.devcel.2013.12.019.

45. Westermann B. 2010. Mitochondrial fusion and fission in cell life and death. Nat Rev Mol Cell Biol 11:872–884. https://doi.org/10.1038/nrm3013.

46. Willems PH, Rossignol R, Dieteren CE, Murphy MP, Koopman WJ. 2015. Redox homeostasis and mitochondrial dynamics. Cell Metab 22:207–218. https://doi.org/10.1016/j.cmet.2015.06.006.

47. Distelmaier F, Valsecchi F, Forkink M, van Emst-de Vries S, Swarts HG, Rodenburg RJ, Verwiel ET, Smeitink JA, Willems PH, Koopman WJ. 2012. Trolox-sensitive reactive oxygen species regulate mitochondrial morphology, oxidative phosphorylation and cytosolic calcium handling in healthy cells. Antioxid Redox Signal 17:1657–1669. https://doi.org/10.1089/ars.2011.4294.

48. Fukui K. 2016. Reactive oxygen species induce neurite degeneration before induction of cell death. J Clin Biochem Nutr 59:155–159. https://doi.org/10.3164/jcbn.16-34.

49. Tardiolo G, Bramanti P, Mazzon E. 2018. Overview on the effects of N-acetylcysteine in neurodegenerative diseases. Molecules 23:3305. https://doi.org/10.3390/molecules23123305.

50. Elbini Dhouib I, Jallouli M, Annabi A, Gharbi N, Elfazaa S, Lasram MM. 2016. A minireview on N-acetylcysteine: an old drug with new approaches. Life Sci 151:359–363. https://doi.org/10.1016/j.lfs.2016.03.003.

51. Wright DJ, Renoir T, Smith ZM, Frazier AE, Francis PS, Thorburn DR, McGee SL, Hannan AJ, Gray LJ. 2015. N-Acetylcysteine improves mitochondrial function and ameliorates behavioral deficits in the R6/1 mouse model of Huntington's disease. Transl Psychiatry 5:e492. https://doi.org/10.1038/tp.2014.131.

52. Arakawa M, Ito Y. 2007. N-acetylcysteine and neurodegenerative diseases: basic and clinical pharmacology. Cerebellum 6:308–314. https://doi.org/10.1080/14734220601142878.

53. Gosalvez M. 2013. Mitochondrial filamentation: a therapeutic target for neurodegeneration and aging. Am J Alzheimers Dis Other Demen 28:423–426. https://doi.org/10.1177/1533317513494451.

54. Fivenson EM, Lautrup S, Sun N, Scheibye-Knudsen M, Stevnsner T, Nilsen H, Bohr VA, Fang EF. 2017. Mitophagy in neurodegeneration and aging. Neurochem Int 109:202–209. https://doi.org/10.1016/j.neuint.2017.02.007.

55. Kallianpur KJ, Walker M, Gerschenson M, Shikuma CM, Gangcuangco LMA, Kohorn L, Libutti DE, Nir TM, Jahanshad N, Thompson PM, Paul R. 2020. Systemic mitochondrial oxidative phosphorylation protein levels correlate with neuroimaging measures in chronically HIV-infected individuals. AIDS Res Hum Retroviruses 36:83–91. https://doi.org/10.1089/AID.2019.0240.

56. Cenini G, Lloret A, Cascella R. 2019. Oxidative stress in neurodegenerative diseases: from a mitochondrial point of view. Oxid Med Cell Longev 2019:2105607. https://doi.org/10.1155/2019/2105607.

57. Bhatti JS, Bhatti GK, Reddy PH. 2017. Mitochondrial dysfunction and oxidative stress in metabolic disorders - A step towards mitochondria based therapeutic strategies. Biochim Biophys Acta Mol Basis Dis 1863:1066–1077. https://doi.org/10.1016/j.bbadis.2016.11.010.

58. Roederer M, Ela SW, Staal FJ, Herzenberg LA, Herzenberg LA. 1992. N-acetylcysteine: a new approach to anti-HIV therapy. AIDS Res Hum Retroviruses 8:209–217. https://doi.org/10.1089/aid.1992.8.209.

59. Xiao H, Neuveut C, Tiffany HL, Benkirane M, Rich EA, Murphy PM, Jeang KT. 2000. Selective CXCR4 antagonism by Tat: implications for in vivo expansion of coreceptor use by HIV-1. Proc Natl Acad Sci U S A 97:11466–11471. https://doi.org/10.1073/pnas.97.21.11466.

60. Gilbert M, Kirihara J, Mills J. 1991. Enzyme-linked immunoassay for human immunodeficiency virus type 1 envelope glycoprotein 120. J Clin Microbiol 29:142–147. https://doi.org/10.1128/JCM.29.1.142-147.1991.

61. Oh SK, Cruikshank WW, Raina J, Blanchard GC, Adler WH, Walker J, Kornfeld H. 1992. Identification of HIV-1 envelope glycoprotein in the serum of AIDS and ARC patients. J Acquir Immune Defic Syndr (1988) 5:251–256.

62. Klasse PJ, Moore JP. 2004. Is there enough gp120 in the body fluids of HIV-1-infected individuals to have biologically significant effects? Virology 323:1–8. https://doi.org/10.1016/j.virol.2004.03.003.

63. Cummins NW, Rizza SA, Badley AD. 2010. How much gp120 is there? J Infect Dis 201:1273–1274; reply 1274–1275. https://doi.org/10.1086/651434.

64. Dringen R, Hamprecht B. 1999. N-Acetylcysteine, but not methionine or 2-oxothiazolidine-4-carboxylate, serves as cysteine donor for the synthesis of glutathione in cultured neurons derived from embryonal rat brain. Neurosci Lett 259:79–82. https://doi.org/10.1016/s0304-3940(98)00894-5.

65. Chen L, Liu L, Yin J, Luo Y, Huang S. 2009. Hydrogen peroxide-induced neuronal apoptosis is associated with inhibition of protein phosphatase 2A and 5, leading to activation of MAPK pathway. Int J Biochem Cell Biol 41:1284–1295. https://doi.org/10.1016/j.biocel.2008.10.029.

66. Hsiao YH, Chen PS, Yeh SH, Lin CH, Gean PW. 2008. N-Acetylcysteine prevents beta-amyloid toxicity by a stimulatory effect on p35/cyclin-dependent kinase 5 activity in cultured cortical neurons. J Neurosci Res 86:2685–2695. https://doi.org/10.1002/jnr.21710.

67. Van Laar VS, Roy N, Liu A, Rajprohat S, Arnold B, Dukes AA, Holbein CD, Berman SB. 2015. Glutamate excitotoxicity in neurons triggers mitochondrial and endoplasmic reticulum accumulation of Parkin, and, in the presence of N-acetyl cysteine, mitophagy. Neurobiol Dis 74:180–193. https://doi.org/10.1016/j.nbd.2014.11.015.

68. Unnithan AS, Jiang Y, Rumble JL, Pulugulla SH, Posimo JM, Gleixner AM, Leak RK. 2014. N-Acetyl cysteine prevents synergistic, severe toxicity from two hits of oxidative stress. Neurosci Lett 560:71–76. https://doi.org/10.1016/j.neulet.2013.12.023.

69. Badisa RB, Wiley C, Randell K, Darling-Reed SF, Latinwo LM, Agharahimi M, Soliman KFA, Goodman CB. 2019. Identification of cytotoxic markers in methamphetamine treated rat C6 astroglia-like cells. Sci Rep 9:9412. https://doi.org/10.1038/s41598-019-45845-1.

70. Avramut M, Zeevi A, Achim CL. 2001. The immunosuppressant drug FK506 is a potent trophic agent for human fetal neurons. Brain Res Dev Brain Res 132:151–157. https://doi.org/10.1016/s0165-3806(01)00307-8.

71. Teodorof C, Divakar S, Soontornniyomkij B, Achim CL, Kaul M, Singh KK. 2014. Intracellular mannose binding lectin mediates subcellular trafficking of HIV-1 gp120 in neurons. Neurobiol Dis 69:54–64. https://doi.org/10.1016/j.nbd.2014.05.002.

72. Hammond RR, Iskander S, Achim CL, Hearn S, Nassif J, Wiley CA. 2002. A reliable primary human CNS culture protocol for morphological studies of dendritic and synaptic elements. J Neurosci Methods 118:189–198. https://doi.org/10.1016/s0165-0270(02)00126-7.